ESync: An Energy Synchronized Charging Protocol for Rechargeable Wireless Sensor Networks

Liang He
Singapore University of Technology and Design
he_liang@sutd.edu.sg

Lingkun Fu*
Zhejiang University, China
lkfu@iipc.zju.edu.cn

Likun Zheng
University of California, Irvine
likunz@uci.edu

Yu Gu
Singapore University of Technology and Design
jasongu@sutd.edu.sg

Peng Cheng, Jiming Chen
Zhejiang University, China
{jmchen}@iipc.zju.edu.cn

Jianping Pan
University of Victoria, Canada
pan@uvic.ca

ABSTRACT

Different from energy harvesting which generates dynamic energy supplies, the mobile charger is able to provide stable and reliable energy supply for sensor nodes, and thus enables sustainable system operations. While previous mobile charging protocols either focus on the charger travel distance or the charging delay of sensor nodes, in this work we propose a novel *Energy Synchronized Charging* (ESync) protocol, which simultaneously reduces both of them. Observing the limitation of the *Traveling Salesman Problem* (TSP)-based solutions when nodes energy consumptions are diverse, we construct a set of nested TSP tours based on their energy consumptions, and only nodes with low remaining energy are involved in each charging round. Furthermore, we propose the concept of energy synchronization to synchronize the charging requests sequence of nodes with their sequence on the TSP tours. Experiment and simulation demonstrate ESync can reduce charger travel distance and nodes charging delay by about 30% and 40% respectively.

1. INTRODUCTION

To address the energy constraints of sensor nodes [1–6], the concepts and implementations of adopting mobile chargers to replenish nodes energy supply in rechargeable sensor networks have attracted a lot of attentions in the research community recently [7–12]. Different from traditional energy harvesting sensor networks [13–17], where the harvested energy is dynamic in both the spatial and temporal dimensions, the mobility-assisted energy replenishment provides a stable and reliable energy supply for sensor nodes and thus enables truly sustainable operations of sensor networks [18–20].

Due to the limited mobility of the charger, the scheduling of charging tasks for sensor nodes in the network plays a critical role in achieving a high charging efficiency. The *Traveling Salesman Problem* (TSP)-based charging protocols are a family of classic solutions to the mobile charging problem [10, 18, 21], with which in general, the mobile charger *periodically* carries out the charging process following a *pre-optimized* tour. As a result, the charging of nodes can be accomplished with a short charger travel distance and thus a short time duration.

However, the limitation of TSP-based solutions is that when nodes energy consumptions are diverse, it may lead to the unnecessary visits of energy-sufficient nodes. This not only increases the charger travel distance when performing the charging tasks of sensor nodes, but also prolongs the waiting time before the energy-hungry nodes can be charged. To address this issue, in this paper, we investigate the on-demand mobile charging scenario where nodes are charged only when necessary. Specifically, sensor nodes send out charging requests to the mobile charger when their energy levels are low, and the charger replenishes their energy supply according to those received requests. We aim to design a novel mobile charging protocol that is able to leverage on the advantages of existing designs while minimizing the impact of their limitations.

The most significant feature in our design is *synchronizing the energy supply of sensor nodes based on a set of nested TSP tours*. Upon achieving such energy synchronization, we can realize the ideal mobile charging paradigm that the charger can simply travel according to the TSP tours to reduce its travel distance, and whenever a sensor node runs short of energy, the charger will *happen to* be traveling towards it. Our major intellectual contributions in this paper are three-fold:

- To the best of our knowledge, our work is the first to jointly improve the charging process for both sensor nodes and the mobile charger, while existing designs only adopt either one of them as the design objective.
- At the macro-level of the mobile charging process, to leverage the advantage of the TSP-based solutions while minimizing the impact of their limitations when node energy consumptions are highly diverse, we construct a set of nested TSP tours based on the energy consumption rates of sensor nodes. Then for each round of the charging process, a novel tour selection algorithm is designed to only involve the energy-hungry nodes into the charging schedule during that round.
- At the micro-level focusing on the charging schedule during individual rounds, observing that nodes charging requests

*The first two authors contributed equally to this work.

MobiHoc'14, August 11–14, 2014, Philadelphia, PA, USA.

http://dx.doi.org/10.1145/2632951.2632970.

sequence may significantly affect the charging performance, we propose the concept of *energy synchronization* among nodes to proactively match nodes charging requests sequence to the selected TSP tour in each charging round, which is achieved by carefully selecting the node to be charged next and controlling the amount of energy charged to individual nodes. As a result, both the charger travel distance and the charging delay of sensor nodes are reduced.

- We evaluate the performance of *ESync* through both experiment and simulations, and the results demonstrate that *ESync* can reduce the charger travel distance and charging latency by 30% and 40% respectively.

The paper is organized as follows. Section 2 briefly reviews the literature. We introduce the problem statement in Section 3. Our design on the nested TSP tours is presented in Section 4, and the design on the energy synchronization among nodes is introduced in Section 5. Section 6 and Section 7 present the evaluation results obtained through both experiment and simulations, and we conclude in Section 8.

2. RELATED WORK

The mobility-assisted energy replenishment provides stable and reliable energy supply for sensor nodes, and has attracted increasing attentions from the research community recently [7–10,18–21]. The mobile charging process can be evaluated from the perspective of the charger and sensor nodes respectively. For the charger, the optimization objective is to minimize its travel distance when performing the charging tasks [9, 20]. The most intuitive approach is to periodically charge nodes along an optimal TSP tour constructed based on network deployment [10]. The idea is extended to the case of charging multiple nodes simultaneously in [18].

Several other designs tackle the mobile charging problem from the perspective of individual sensor nodes [7, 8, 22]. A scheme jointly exploring the routing and charging of individual nodes is proposed in [7], which proactively guides the routing activities in the network and delivers energy to where it is needed. A greedy charging algorithm that always charges the node with the shortest remaining lifetime to its full capacity is proposed in [8], and is further improved by incorporating the remaining energy levels of other nodes when determining which node to charge next and how much energy to charge to. Another way to greedily performing the charging tasks is to always select the nearest requesting node to charge, i.e., the Nearest-Job-Next discipline. The performance of Nearest-Job-Next is analytically evaluated in [23, 24]. Although asymptotically promising, the worst-case performance of Nearest-Job-Next is difficult to guarantee.

With the concept of energy synchronization among nodes based on a set of nested TSP tours, we propose a novel mobile charging protocol that leverages on the advantages of both the existing designs while minimizing the impact of their drawbacks. Our design reduces the charger travel distance by scheduling based on the nested TSP tours, and reduces the charging delay of sensor nodes with the concept of energy synchronization within each round of selected tours.

3. PRELIMINARIES

3.1 Problem Statement

With the advancement of the energy transferring technologies, the time to replenish the energy supply of sensor nodes has been dramatically reduced [20,25]. Zhu et al. have implemented an energy sharing system with capacitor-array powered sensor nodes [17], in which the energy supply in the network is transferred from energy-sufficient nodes to energy-hungry nodes. From the empirical results reported in [16], the time to charge a $10\ F$ capacitor from empty to a voltage of $2.5\ V$ is in the order of $10\ s$ normally. This greatly shortened charging time indicates that adopting mobile chargers to replenish nodes energy supply is a promising direction for stable and sustainable network operations.

In this work, we investigate the on-demand mobile charging problem in rechargeable sensor networks, where a mobile energy charger travels within the deployment field, and replenishes the energy supply of nodes via short-distance or direct-contact charging technologies such as *inductive charging* [26]. The mobile charger is controllable in both its travel trajectory and the amount of energy charged to individual sensor nodes.

When the remaining energy levels of sensor nodes are low, the nodes initiate charging requests to the mobile charger either by the communications (potentially in multiple hops) between themselves and the charger [27,28] or with the assistance of a sink [7,8] [1]. Our objective is to design an efficient mobile charging protocol for the charger to effectively serve the received charging requests. Here by *serving* a charging request, we mean the charger travels to the requesting sensor node and replenishes its energy supply to the desired level. The mobile charging process can be evaluated from two aspects.

• **Charging Delay** For the requesting sensor nodes, the charging process is evaluated based on their *charging delay*, defined as the time since they send out their charging requests to the time their energy is replenished by the charger. A shorter charging delay implies a higher charging efficiency.

• **Charger Travel Distance** For the mobile charger, the charging efficiency is evaluated in terms of its *travel distance* to carry out the charging tasks of nodes. A shorter travel distance indicates a higher charging efficiency.

Most existing works choose only one of the two aspects above as the design objective. For example, reducing the charging latency of sensor nodes is emphasized in [7,8,22], while the charging process is optimized by shortening the charger travel distance in [10,18]. To the best of our knowledge, our work is the first attempt to jointly tackle these two objectives.

3.2 State-of-the-Art and Limitations

The TSP-based solutions are a classic family of the designs on the mobile charging problem [10,18,21]. In general, with the TSP-based solutions, the mobile charger *periodically* travels along a pre-optimized TSP tour to replenish the energy supply of nodes in each round of the charging process, and thus the charger travel distance in replenishing the energy of all nodes is minimized. However, to take advantage of the pre-optimized TSP tour in the on-demand mobile charging scenario, there are two facts that would significantly degrade the charging performance.

3.2.1 Diversity in Nodes Energy Consumption

The efficiency of the TSP-based solutions degrades when nodes energy consumption rates are highly diverse, which is unfortunate-

[1]A remaining energy level threshold can be adopted for sensor nodes to initiate their charging requests. For the ease of description, we assume a threshold of 0% in this paper. Furthermore, as both the time for the charger to travel to the requesting node and the time to replenish nodes energy supply are normally much longer than the communication delay, we assume a negligible time to deliver charging requests from nodes to the charger, similar to [29].

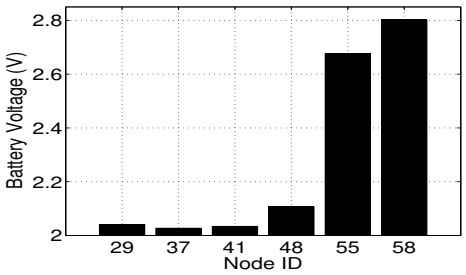

Figure 1: Diverse nodes remaining energy (original data is provided by [30]).

ly true in most cases for multihop sensor networks [29]. The high energy consumption diversity may cause highly diverse nodes remaining energy levels, and as a result, traveling along the pre-optimized tour leads to the unnecessary visits of energy-sufficient nodes. This not only increases the charger travel distance but also prolongs the charging delay of energy-hungry nodes.

To clearly demonstrate the potentially unnecessary visits of energy-rich nodes, Figure 1 presents the voltage readings of six sensors at a specific time in a data trace provided by Intel Berkeley Research Lab, which is collected with the granularity of 1 second between February 28th and April 5th, 2004 [30]. We can observe the obvious voltage diversity among the nodes. In this case, if the charger carries out the charging process based on the TSP tour constructed according to these six nodes, it would arrive at node-55 and node-58 only to find out that they have little demand for energy replenishment.

3.2.2 Sequence of Nodes Charging Requests

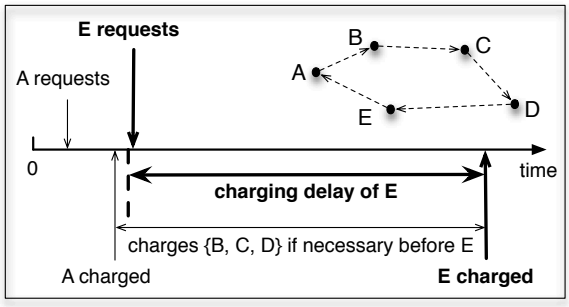

Figure 2: Requests sequence affects the charging performance significantly: the charging delay of E is long if E requests charging when the charger has already passed it in the current charging round.

Furthermore, in the on-demand charging scenario, even if nodes have similar energy consumptions, indicating they may all need to be charged in a given round, their charging requests sequence plays a critical role in determining the performance of the periodic charging process, which must be considered if we want to utilize the advantage of the TSP-based solutions in minimizing the charger travel distance. Figure 2 demonstrates an example on how the charging requests sequence affects the charging performance. Consider the network shown in the upper-right corner of the figure, where the charger periodically carries out the charging tasks according to the optimal TSP tour shown with the dashed lines. If node E requests charging when the charger has just charged A, meaning the charger has already passed E in this round, the charger would first charge

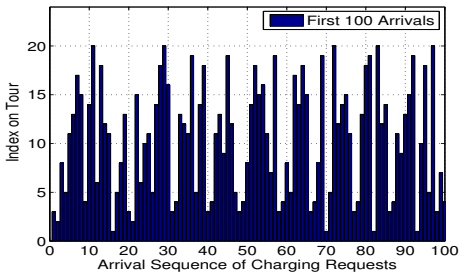

Figure 3: Requests sequence mismatches nodes sequence along the tour.

node B, C, and D if necessary. In this way, the energy of E will not be replenished until the charger reaches it in the next round, which leads to a large charging delay of E.

The fundamental reason for E's long charging delay in the above example is that the charging requests sequence mismatches with the node sequence on the optimal TSP tour. To examine whether the mismatching between the two sequences exists in practice, we simulate a small environment monitoring sensor network consisting of 20 sensor nodes with similar energy consumptions. We construct a near-optimal TSP tour based on the nodes deployment with the open source TSP solver *Concorde* [31], and index nodes according to their sequence along the tour. We record the charging requests sequence of nodes, and the first 100 requests are shown in Fig. 3. We can see the indexes of requesting nodes are quite random with regard to the nodes requesting sequence, which would lead to the undesired case shown in Fig. 2.

It is possible to avoid the undesired case shown in Fig. 2 by removing the periodic property from the charging process, e.g., performing charging tasks according to the classic Nearest-Job-Next discipline [23]. However, removing the periodic property may lead to the *zig-zag* travel of the charger and cause unfairness issue among sensor nodes. Our evaluation results show that our design outperforms Nearest-Job-Next by about 30%-40%, as will be explained in Section 6 and Section 7.

3.3 Design Overview

In this paper, focusing on the scenario where the energy consumption rates are diverse among sensor nodes, we propose the *Energy Synchronized Charging* (*ESync*) protocol, which addresses the above two limitations by first *constructing a set of nested TSP tours* and then *synchronizing nodes energy according to the tours*. The motivation of the nested TSP tours is to only involve nodes with low remaining energy levels in each charging round to reduce the charger travel distance. The motivation for the energy synchronization among nodes is to proactively adjust nodes charging requests sequence to synchronize it with the TSP tour selected in each round, and thus reduce the charging delay of sensor nodes.

4. CONSTRUCTION OF NESTED TOURS

The limitation of the TSP-based solutions with diverse node energy consumptions inspires us to cluster nodes according to their energy consumption rates, and then based on these clusters, we construct multiple TSP tours in a *nested* manner. We further present a corresponding tour selection algorithm to guide the charging process in each round.

4.1 Nodes Clustering

Before introducing the design of our clustering algorithm, we first use a simplified example as shown in Fig. 4 to present our

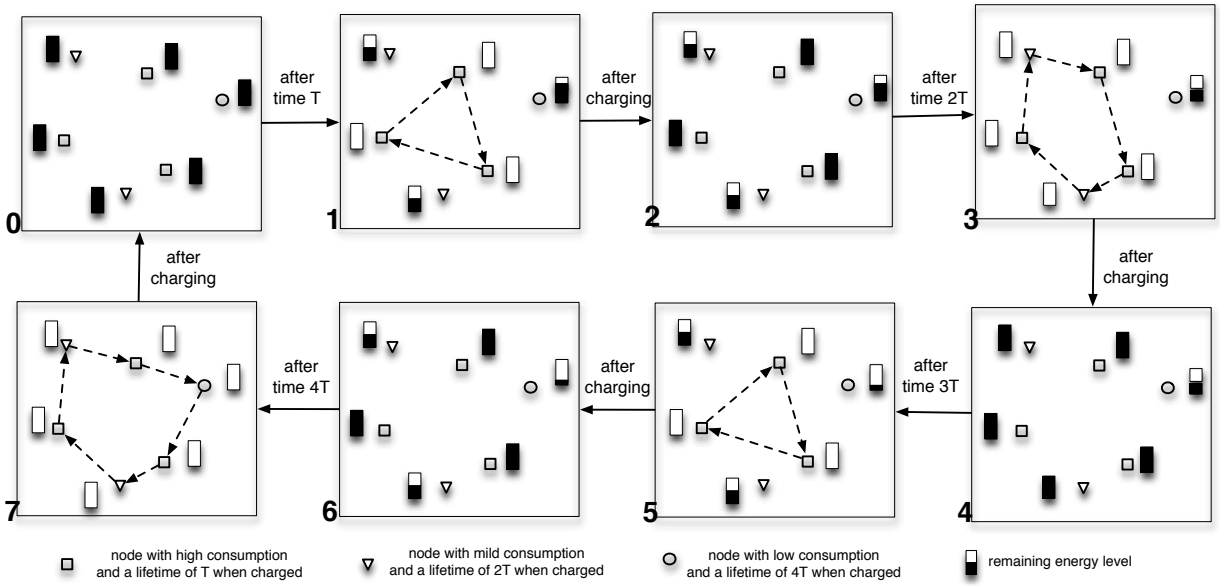

Figure 4: Clustering nodes according to their energy consumption rates, and then a set of nested TSP tours is constructed. One of these TSP tours is selected to guide the charging tasks in each charging round.

idea. The energy consumption rates of nodes represented by the squares are twice of the triangle nodes and four times of the circle nodes. Denote the lifetime of square nodes when fully charged by T. Consequently, the triangle and circle nodes have a $2T$ and $4T$ lifetime when fully charged, respectively [2].

If we take these three categories of nodes as three clusters, then when the square nodes deplete their energy after an operation time of T, the charger only needs to charge the square cluster as both the triangle and circle nodes still have sufficient energy supply (Fig. 4(1)). The nodes remaining energy levels after the charging of the square nodes are shown in Fig. 4(2) [3]. After another operation time of T, both the square and triangle nodes deplete their energy, and this time the charger needs to charge the two corresponding clusters as shown in Fig. 4(3). When an operation time of $4T$ is passed, the charger needs to replenish the energy supply of all nodes, as shown in Fig. 4(7), and the process repeats afterwards.

In this example, the nodes clusters can accurately separate the energy-hungry nodes from the energy-rich nodes in each charging round, and thus the charger only needs to consider the nodes clusters, instead of individual nodes, to carry out the charging process. The fundamental property leads to this effect is that nodes in the same cluster have similar energy consumptions. Based on this observation, we propose a novel *power-*α clustering algorithm to group nodes according to their energy consumptions.

Assume all nodes are initially fully charged, we begin our design from the time that at least one charging request has been received from each node. This ensures the charger has certain knowledge on the energy consumption conditions of all nodes, based on which the estimation on their energy consumption rates is feasible [32]. The charger can adopt any existing charging protocols before this time [7, 23, 24].

Denote $r_{\max}$ and $r_{\min}$ as the maximal and minimal nodes energy consumption rate, respectively. We construct a total number of m intervals and

$$m = \lceil \log_\alpha (\frac{r_{\max}}{r_{\min}}) \rceil^+, \quad (1)$$

where $\lceil x \rceil^+$ returns the first integer that is larger than x [4], and α is an integer design parameter that is larger than 1. With the ascending order of energy consumption rates, these m intervals are: $[r_{\min}, \frac{r_{\max}}{\alpha^{m-1}}]$, $(\frac{r_{\max}}{\alpha^{m-1}}, \frac{r_{\max}}{\alpha^{m-2}}]$, $\cdots$, $(\frac{r_{\max}}{\alpha^2}, \frac{r_{\max}}{\alpha^1}]$, $(\frac{r_{\max}}{\alpha^1}, r_{\max}]$. Note that the length of each interval increases exponentially with α. For each node s, it is clustered into the i-th cluster if its energy consumption rate $r(s)$ falls into the i-th interval. For example, if $r_{max} = 6$, $r_{min} = 1$, and $\alpha = 2$, then $m = \lceil \log_2 \frac{6}{1} \rceil^+ = 3$ intervals are constructed. The three intervals are $[1, 1.5]$, $(1.5, 3]$, and $(3, 6]$, respectively. For clarity, we refer to the interval with the highest consumption rate (i.e., $(3, 6]$) as the 1-st interval and the corresponding cluster as the 1-st cluster. Similarly, the interval $(1.5, 3]$ and $[1, 1.5]$ are referred to as the 2-nd and 3-rd intervals, and the corresponding clusters as the 2-nd and 3-rd clusters, respectively.

With this clustering approach, the ratio between the maximal and the minimal energy consumption rates of nodes in the same cluster is upper bounded by α. Clearly, α plays a critical role in determining the charging performance. We will elaborate the optimal setting of α in Section 4.4, and our evaluation results in Section 7 indicate that an α of 2 leads to the best performance in most cases.

Note that in event-driven sensor network applications such as target tracking, the energy consumption rates of individual sensor nodes may vary over time. In this case, we need to dynamically adjust the clustering of nodes (and the constructed TSP tours as will be introduced below) to guarantee the energy similarity of nodes in the same cluster. An important observation on these event-driven

[2]To highlight the motivation of our design, the nodes energy consumption rates in this example are intentionally set to be diverse. However, our design is also applicable to scenarios where nodes have similar energy consumptions.

[3]The time to finish the charging of these nodes is assumed to be negligible for the ease of demonstration, which is further investigated in Section 7.

[4]Note its difference with the traditional operator $\lceil x \rceil$ when x is an integer.

applications is that although the energy consumptions for individual nodes may not be constant, their activities demonstrate certain periodicity and predicability [33], which can be used to dynamically adjust the clustering of sensor nodes.

4.2 Nested Tour Construction

The next step is to construct TSP tours according to the m clusters in a nested manner. We construct m TSP tours based on the first i clusters ($i = 1, 2, \cdots, m$), and denote these tours as $\{T^1_{tsp}, T^2_{tsp}, \cdots, T^m_{tsp}\}$. Because the tours are constructed in a nested manner, their length satisfies the following relationship

$$|T^1_{tsp}| \leq |T^2_{tsp}| \leq |T^3_{tsp}| \leq \cdots \leq |T^m_{tsp}|. \quad (2)$$

In the example shown in Fig. 4, three nested TSP tours are constructed based on these three nodes clusters. The shortest tour T^1_{tsp} is shown in Fig. 4(1), the second shortest tour T^2_{tsp} is shown in Fig. 4(3), and the longest tour T^3_{tsp} is shown in Fig. 4(7).

4.3 Tour Selection for Each Round

With the nested TSP tours, the mobile charger periodically carries out the charging tasks by selecting one of these nested tours in each round, and charges the nodes involved in the tour if necessary. Thus, the next question we need to decide is which tour the mobile charger should select for a given round of the on-demand charging process.

4.3.1 Key Observation

Again, before introducing our design on the tour selection algorithm, we first use the example shown in Fig. 4 to present our basic idea. With the *Power-*α clustering algorithm and the tour construction method introduced above, we obtain three node clusters (i.e., square, triangle, and circle) and three nested TSP tours (i.e., T^1_{tsp}, T^2_{tsp}, and T^3_{tsp} as in Fig. 4(1), Fig. 4(3), and Fig. 4(7)). For the mobile charger, it is desirable to select the shortest TSP tour containing all the energy depleted nodes in each charging round. In the 1-st round of the charging process, only the square nodes deplete their energy supply, and thus the charger would prefer to select the shortest tour containing the square nodes, i.e., T^1_{tsp}, as the tour to guide the charging process (Fig. 4(1)). Similarly, in the 2-nd round, the charger would prefer to select the shortest tour containing the square and triangle nodes, i.e., T^2_{tsp}, to follow (Fig. 4(3)). T^1_{tsp} is selected again in the 3-rd round since now only the square nodes are out of energy supply (Fig. 4(5)). Then in the 4-th round, all nodes deplete their energy supply, and the TSP tour containing all of them is selected (Fig. 4(7)). From this example, we can see the tour selection algorithm is expected to identify the shortest TSP tour containing all the energy-hungry nodes in each charging round, and the following observation inspires us the solution.

For any given α and m, every $j \in \{0, 1, \cdots, \alpha^{m-1}\}$ can be represented in the form of

$$j = \sum_{i=0}^{m-1} c_i^j \cdot \alpha^i, \quad (3)$$

where $c_i^j \in \{0, 1, \cdots, \alpha - 1\}$. To clearly demonstrate the relationship between the selected tour in j-th round and j's sum expression in (3), let us define an ordered set $\mathcal{C}_j = <c_0^j, c_1^j, \cdots, c_{m-1}^j>$. For the ease of description, further define $\mathcal{C}_0 = <0, 0, \cdots, 0>$ and $|\mathcal{C}_0| = m - 1$. Then with $\alpha = 2$ and $m = 3$, the sum expressions and the corresponding $\mathcal{C}_j$ for the first four rounds of the mobile charging process are shown in Fig. 5.

We can see that in the 1-st round, the only element in $\mathcal{C}_1$ that is larger than the corresponding element in $\mathcal{C}_0$ is the 1-st element,

$$\begin{aligned}
0 &= 0 \times 2^0 + 0 \times 2^1 + 0 \times 2^2 &\rightarrow\ & \mathcal{C}_0 = <0, 0, 0>, \\
1 &= 1 \times 2^0 + 0 \times 2^1 + 0 \times 2^2 &\rightarrow\ & \mathcal{C}_1 = <1, 0, 0>, \\
2 &= 0 \times 2^0 + 1 \times 2^1 + 0 \times 2^2 &\rightarrow\ & \mathcal{C}_2 = <0, 1, 0>, \\
3 &= 1 \times 2^0 + 1 \times 2^1 + 0 \times 2^2 &\rightarrow\ & \mathcal{C}_3 = <1, 1, 0>, \\
4 &= 0 \times 2^0 + 0 \times 2^1 + 1 \times 2^2 &\rightarrow\ & \mathcal{C}_4 = <0, 0, 1>.
\end{aligned}$$

Figure 5: Tour selection based on the sum expression in (3).

and from the example in Fig. 4, we know the 1-st tour (i.e., T^1_{tsp}) is desirable to be selected in the 1-st round. For the second round, the 2-nd element in $\mathcal{C}_2$ is larger than the 2-nd element in $\mathcal{C}_1$, and on the other hand, the second tour T^2_{tsp} is desirable to be selected in the 2-nd round. This agreement holds for the 3-rd and 4-th rounds as well. For the 3-rd round, the 1-st element in $\mathcal{C}_3$ is larger than that in $\mathcal{C}_2$, and the desirable tour is T^1_{tsp}. For the 4-th round, the 3-rd element in $\mathcal{C}_4$ is larger than that in $\mathcal{C}_3$, and the desirable tour is T^3_{tsp}.

This relationship between the tour selected in the j-th round and j's sum expression inspires us the design of the tour selection algorithm.

4.3.2 Tour Selection Algorithm Design

For a given round index $j \in \{1, 2, \cdots, \alpha^{m-1}\}$, we first identify the corresponding $\mathcal{C}_j$. Then we compare it with $\mathcal{C}_{j-1}$, and find the k ($k = 0, 1, \cdots, m-1$) such that c_k^j is larger than c_k^{j-1}. It can be proved that one and only one such k can be found for every round index j, which is not included here due to the space limit. As a result, the charger takes the $(k+1)$-th tour in the j-th round. The sequence of the adopted tours repeats every α^{m-1} rounds.

We can see that with the proposed tour construction and selection algorithms, for each round of the charging process, the charger always selects the shortest TSP tour that contains all the sensor nodes with low remaining energy levels. As a result, the charger travel distance during the charging process is reduced.

4.4 Determining the Optimal Power Factor

We have introduced how to construct the nested TSP tours and which tour to select for each charging round with a given power factor α. Next we explain how to identify the optimal setting of α. The optimal α is jointly determined by nodes energy consumption rates and their locations. This means identifying the optimal α before network deployment is challenging. However, once at least one charging request has been received from each node, both the estimated energy consumption rates and nodes locations can be made available to the charger, e.g., by piggybacking these information in the charging requests, based on which the optimal α can be identified.

For the ease of description, we extend our previous notation on T^i_{tsp} by denoting the i-th TSP tour obtained with a specific α as $T^i_{\text{tsp}(\alpha)}$. Denote m_α as the number of clusters obtained with power factor α. With the proposed tour selection algorithm, the sequence of adopted tours will repeat every $\alpha^{m_\alpha - 1}$ rounds. The worst-case charger travel distance during these rounds Y_α is

$$Y_\alpha = |T^{m_\alpha}_{\text{tsp}(\alpha)}| + \sum_{i=1}^{m_\alpha - 1} \alpha^{m_\alpha - i - 1} |T^i_{\text{tsp}(\alpha)}|,$$

and thus an upper bound Z_α of the asymptotic average travel distance for each round is

$$Z_\alpha = Y_\alpha / (\alpha^{m_\alpha - 1}).$$

Then the mobile charger can adopt the α with the minimum Z_α to carry out the charging tasks

$$\hat{\alpha} = \{\alpha : \min\{Z_\alpha\}\}$$

Note that when $\alpha > \frac{r_{\max}}{r_{\min}}$, only one cluster containing all the nodes will be formed, and *ESync* regresses to the simple case where only the TSP tour containing all nodes is involved in the charging process. Thus the charger only needs to check the potential value of α in $[2, \frac{r_{\max}}{r_{\min}}]$ to determine its optimal setting.

4.5 Time Complexity

We needs a time of $\mathcal{O}(m_\alpha C_{\text{tsp}})$ to accomplish the node clustering and tour construction with a specific α, where C_{tsp} is the time complexity to obtain the near-optimal TSP tour. As mentioned earlier, the charger needs to check at most $(\frac{r_{\max}}{r_{\min}} - 1)$ possible values of α to determine the optimal setting. As a summary, the computation complexity in constructing the nested TSP tours is $\mathcal{O}(C_{\text{tsp}} \frac{r_{\max}}{r_{\min}} \log \frac{r_{\max}}{r_{\min}})$. The charger needs a time of $\mathcal{O}(\log_\alpha \frac{r_{\max}}{r_{\min}})$ to select the tour in each round.

5. ENERGY SYNCHRONIZATION AMONG NODES

With the nested TSP tours and the tour selection method, only energy-hungry nodes are involved in each charging round. In this section, we further improve the charging process by synchronizing the energy supply of nodes to proactively adjust their charging requests sequence. As a result, the charging requests sequence of nodes is synchronized with their sequence on the TSP tours. Specifically, if the charging requests from two neighboring nodes are sent out according to their sequence on the selected TSP tour, we say these two nodes are *energy synchronized* in the charging process. This energy synchronization among nodes is achieved by carefully controlling the amount of energy charged to individual nodes.

In generally, the mobile charger needs to address two questions to carry out the charging process in each round: which node to charge next, and then how much energy to charge to the node.

5.1 Which Node to Charge Next

In our design, the node to be charged next is determined according to the selected TSP tour in each round. Specifically, after completing the charging of the current node, the mobile charger selects the requesting node that is closest to its current location along the TSP tour as the next node to charge.

Although our method demonstrates greedy feature, which may cause the unfairness issue among sensor nodes. Because we only applies the greedy feature based on the TSP tour, the potential unfairness issue is significantly alleviated.

5.2 How Much to Charge

To achieve the energy synchronization among nodes, the charger does not always fully charge individual nodes, and next we explain how to determine the amount of energy charged to the selected node. In our design, we determine the amount of energy charged to individual nodes with the objective of synchronizing their energy supplies. Thus given the selected charging node, we first need to identify the node to which to synchronize its energy, i.e., its *synchronization target*.

Assume the mobile charger is currently working in the j-th round following tour $T_{tsp}^{f(j)}$, where $f(j)$ is the tour index returned by the tour selection algorithm. To find the synchronization target of a given node s in this round, which belongs to the i-th cluster, we first identify the round j' in which s is involved the next time by

$$j' = j + \alpha^{i-1} \quad (i = 1, 2, \cdots, m). \tag{4}$$

The adopted tour in the j'-th round, $T_{tsp}^{f(j')}$, can be calculated by the tour selection algorithm. Then we find the previous node of s along $T_{tsp}^{f(j')}$ as the synchronization target of s in the j-th round, which is denoted as u for the ease of description. This is because the desired effect we want to achieve is when s requests energy replenishment the next time, the mobile charger has just accomplished the charging of u in the j'-th round, meaning the energy of s is synchronized with u in the j'-th round.

Two pieces of information are needed to calculate the amount of charged energy to achieve the energy synchronization between s and u: the energy consumption rates of s and u, and the time duration until u is charged in the j'-th round.

The nodes energy consumption rates can be estimated based on the history of charging requests. As an example, the energy consumption rate of a specific node can be estimated based on its operation time with a single full charging [32]. We emphasize that the perfect estimation is extremely challenging. Our design does not require the perfect estimation of nodes energy consumption rates, and we will further discuss and investigate the charging performance under varying estimation errors in Section 7. Through our extensive simulation, we observe that our design can tolerate up to 30% estimation errors, which can be easily guaranteed by the state-of-the-art power monitoring solutions [34, 35].

Next we explore the time duration until u is charged in the j'-th round. The number of rounds that u is involved between the j-th and j'-th round can be calculated in a similar manner as (4), and denote it as q. The total amount of energy charged to u in these q rounds is at most qE, and thus the time from now till u requests charging in the j'-th round is at most $\frac{qE+e_r(u)}{r(u)}$, where $e_r(u)$ is the current remaining energy of u and $r(u)$ is its energy consumption rate.

As a result, the amount of energy charged to s is calculated according to

$$e(s) = r(s)\left(\frac{qE + e_r(u)}{r(u)} + t_c\right) - e_r(s), \tag{5}$$

where t_c is the worst-case charging time to fully replenish nodes energy supply (i.e., the longest possible time to charge u in the j'-th round), and thus $(\frac{qE+e_r(u)}{r(u)} + t_c)$ is the time before the charger arrives to charge s the next time. Note that $e(s) \in [0, E - e_r(s)]$.

Determining the amount of charged energy according to (5) indicates that the charger would not always fully charge individual nodes. However, this occasionally partially charging of nodes facilities the energy synchronization among nodes, and thus the overall charging performance outperforms that when the charger always fully charge nodes. Specifically, from our evaluation results in Section 7, we observe a 30% and 40% reduction in the charger travel distance and the charging delay of sensor nodes, respectively.

During the charging process in each round, the charger needs a time of $\mathcal{O}(n)$ to determine the next node to charge, and another time of $\mathcal{O}(\log_\alpha \frac{r_{\max}}{r_{\min}})$ is needed to determine the amount of charged energy.

5.3 Charger Energy Replenishment

Although usually the mobile charger has a much larger energy capacity than sensor nodes, the energy replenishment of the charger itself also needs to be considered in practical implementations, especially when the deployment field or the number of deployed nodes is large. *ESync* can seamlessly incorporate the energy replen-

Table 1: Average energy consumption rates.

Node	#1	#2	#3	#4	#5	#6	#7	#8	#9
r_i	4	2	4	2	1	4	1	4	2

Table 2: Scale-down a realistic network for the experiment

	Envisioned Network	Experiment
Network Area	$1,000 \times 1,000\ m^2$	$3 \times 3\ m^2$
Nodes Lifetime	10–40 hours	100–400 s
Fully Charge Time	20 min	3.33 s

ishment of the charger into the charging process. Assume there is an energy tank from which the charger energy can be replenished. Whenever the energy level of the charger is low, we treat it as a *virtual charging request* initiated by the energy tank. The energy tank can be included into the nested tours construction based on the charger's operation time with a single charge, just as a usual sensor node. As a result, the charger's energy replenishment can be handled in the same way as the sensor nodes.

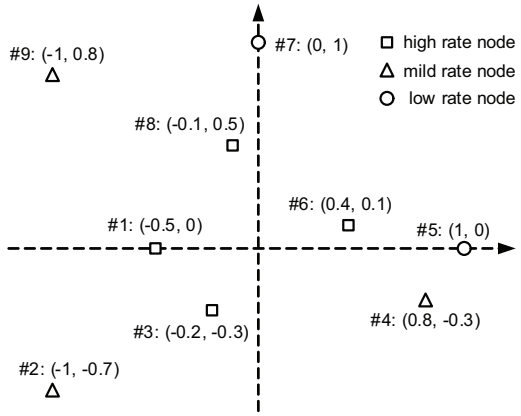

Figure 6: Nodes locations.

6. EXPERIMENT EVALUATION

We evaluate the performance of *ESync* through both experiments and simulations. The experiment results are presented in this section, and the insights obtained through large-scale simulations will be introduced in the next section.

In our experiment, we randomly deploy 9 sensor nodes in an open field of $3\times3\ m^2$, and a LEGO Mindstorms NXT robot with an average travel speed of $0.1\ m$ per second is adopted as the mobile charger. The locations of these nodes are shown in Fig. 6.

Figure 8 shows the relationship between battery voltage and the charging time obtained with our empirical measurements. The battery can be rapidly charged in the early charging stage, during which the battery voltage and the charging time demonstrate clear linear relationship (as shown in the box in Fig. 8). However, as the battery approaches its full voltage, the charging speed significantly slows down. Similar charging curves are reported in the data sheets of off-the-shelf battery products [36]. Based on this observation, we implement a simple linear charging model to emulate the charging of nodes. Specifically, the time to accomplish the charging of a specific node s is calculated by $\frac{e(s)}{E}t_c$ where $e(s)$ is the amount of energy charged to s, E is the full energy capacity of nodes, and t_c is the time to fully charge an energy depleted node. This simplified charging model is sufficient for our evaluation purpose, especially when not all the nodes are fully charged in our energy synchronized charging design (which avoids the non-linear portion of the charging curve). Specifically, we emulate a scenario where $E = 100$ units and the charging rate of the charger is 30 units per second, indicating the worst-case charging time $t_c = \frac{100}{30} \approx 3.3$ s. The average energy consumption rates of nodes are shown in Table 1.

The rationale behind these settings is because of our limited testbed size (i.e., $3 \times 3\ m^2$ as stated above), we need to scale-down a realistic network in both the spatial and temporal dimensions. Specifically, we envision a network area of $1,000 \times 1,000\ m^2$ where the average nodes lifetime is about $10 - 40$ hours upon fully charged. The charger needs a charging time of about 20 minutes to fully charge an energy-depleted node, as with the commercial fast charger for AA batteries commonly adopted on sensor nodes. Then we map the considered network area to our experiment field, and scale-down other settings accordingly, as shown in Table 2.

These 9 sensor nodes are organized into 3 clusters based on their energy consumption rates (i.e., $\{1, 3, 6, 8\}$, $\{2, 4, 9\}$, and $\{5, 7\}$), and 3 nested TSP tours are constructed accordingly, as highlighted in Fig. 7. Sensor nodes send out charging requests to the charger when their energy supply is depleted, and the charger carries out these charging tasks according to *ESync*.

We evaluate the performance of *ESync* and compare it with two classic baselines: TSP [24] and Nearest-Job-Next [23], upon which most existing designs are based [10, 18]. For TSP, the charger travels and charges nodes following the TSP tour, and its travel is independent of whether the charging request from the node has been received. For Nearest-Job-Next, the charger always selects the geographically nearest requesting node as the next node to charge. Both these two baselines adopt the full charging of nodes throughout the charging process.

To capture the fact that nodes energy consumption rates are usually dynamic in practice, we introduce an estimation error parameter ϵ to generate the actual energy consumption of nodes in each second. Specifically, the energy consumption of node-i in each second is randomly generated in

$$[(1 - \epsilon)r_i, (1 + \epsilon)r_i], \tag{6}$$

where r_i is the average energy consumption rate of node-i as shown in Table 1. [5]

A mobile charging process of 15 minutes is performed in each experiment, and the requests charging delay and charger travel distance during these charging processes are recorded for evaluation. To better visualize the mobile charging process, Figure 9 shows the recorded charger travel trajectory during a particular experiment. Note that the charger trajectory is not straight lines due to the kinetic constraints.

The charger travel distance and requests charging delay resultant with ϵ varing from 0–30% are shown in Fig. 10 and Fig. 11, respectively. We can see the charger travel distance resultant by *ESync* is about 30% and 20% shorter than those obtained by TSP and Nearest-Job-Next, and the request charging delay is reduced by about 50%. Furthermore, we can see that although the performance of *ESync* degrades with a larger estimation error on nodes energy consumption rates, it still noticeably outperforms both TSP and NJN even with an ϵ as large as 30%, indicating a good tolerance of *ESync* on the energy consumption variance of sensor nodes.

To clearly illustrate the evolution of nodes remaining energy during a mobile charging process of 15 minutes, we show the energy level of node-1, node-2, and node-5 in Fig. 12, one for each of the

[5]However, we assume a perfect estimation on nodes energy consumption rates for TSP and Nearest-Job-Next.

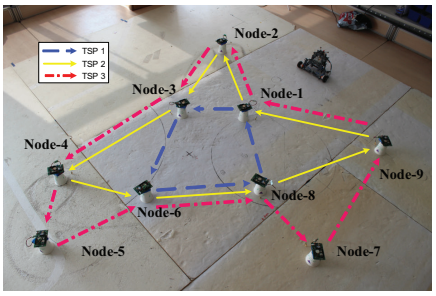

Figure 7: Overview of the experiment settings.

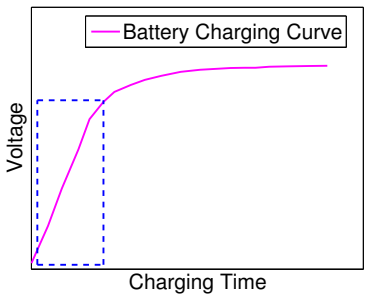

Figure 8: Typical battery charging curve over time.

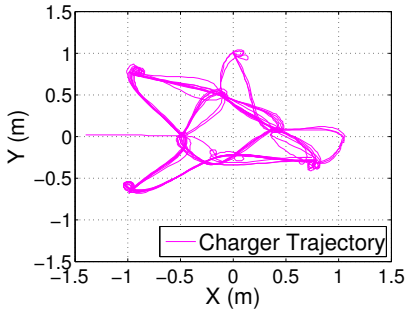

Figure 9: Charger trajectory during the mobile charging process.

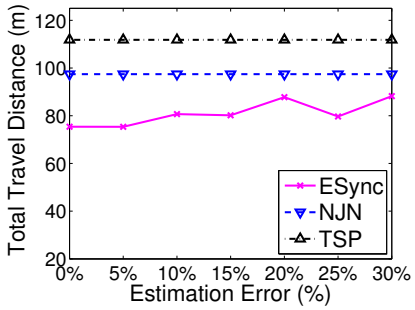

Figure 10: Charger travel distance with estimation error ϵ.

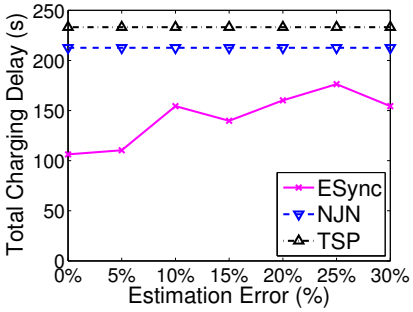

Figure 11: Charging delay with estimation error ϵ.

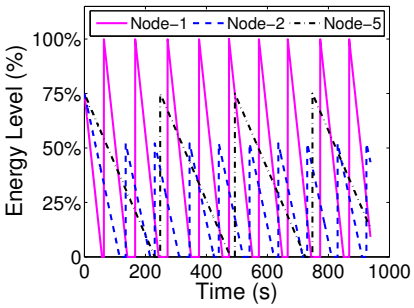

Figure 12: Nodes energy during experiment.

three nodes clusters. We can see node-1 is always charged to its full capacity because it has the highest energy consumption rates (and thus the shortest lifetime) in the network, while node-2 and node-5 are only partially charged. Furthermore, the frequencies for the three nodes to be charged decrease with the order of node-1, node-2, and node-5. This is because node-1 is involved in all three nested TSP tours while node-5 is only involved in the 3rd tour, as shown in Fig. 7.

7. SIMULATION EVALUATION

In this section, we evaluate the performance of *ESync* through extensive simulations.

7.1 Simulation Setup

We simulate an environment monitoring sensor network with 20–200 randomly deployed nodes. The sensing field size varies from 60 $m \times 60$ m to 160 $m \times 160$ m, and a sink is located at the field center. The nodes energy capacity is $1,000$ mAH. The energy consumption rate for the sensing tasks is 0.75 $mA \times 2$ $V = 1.5$ mW, which is typical for a light sensor [37]. The communication energy costs of sensor nodes are set based on the data sheet of MICA2 node: with transmitting and receiving current draw of 25 mA and 8 mA respectively, the corresponding energy consumption rates are $25mA \times 2$ $V = 50mW$ and $8mA \times 2$ $V = 16mW$ with a typical voltage of 2 V. After nodes deployment, a routing structure is constructed based on the TinyOS standard CTP [38]. Then the environment information, after captured by individual nodes, is transmitted to the sink through multi-hop communications. Sensor nodes send out charging requests to the charger when their remaining energy approaches zero. The charger travel speed is 1 m/s unless otherwise specified [29]. We simulate a network operation period of $500,000$ s, and record the total distance the mobile charger traveled and the total charging delay of sensor nodes. We adopt *Concorde* [31], an open source TSP solver with verified efficiency, to obtain the near-optimal TSP tours in our simulation. The mobile charging process is simulated with Matlab.

7.2 Visualizing the Effect of Energy Synchronization

Before evaluating the performance of *ESync*, we first run *ESync* on the same setting as in Fig. 3 to visualize the effect of energy synchronization when only a single TSP tour is constructed. With a simulated time of $500,000$ s, during which a total number of 948 charging requests are served, the last 100 requests in the simulation are shown in Fig. 13. We can see although the realization of energy synchronization is not perfect due to the dynamics in the charging process, the requests sequence greatly matches the TSP tour, and thus our design is validated. Furthermore, we observe that the effect of energy synchronization begins to show as early as from the 200-th to 300-th requests, indicating a short time to achieve the energy synchronization.

7.3 Performance Evaluation

7.3.1 *Impact of Network Scale*

To investigate the scalability of *ESync*, we evaluate its performance with different network scales w.r.t. the number of deployed sensor nodes. The resultant charger travel distance and charging delay of sensor nodes are shown in Fig. 14(a) and Fig. 14(b) respectively, where the number of nodes varies from 20 to 200. Note that due to the large gap among the results returned by the three charging protocols, the y-axis in the figures is in *log-scale*. We can see *ESync* achieves the best performance for all the network scales investigated. For example, the charger travel distance (charging

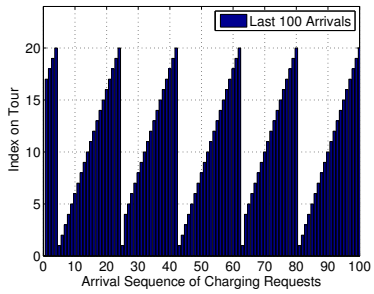

Figure 13: Effect of energy synch.

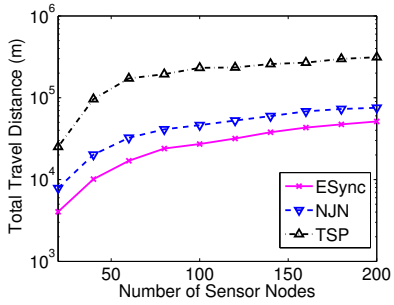

(a) Total travel distance

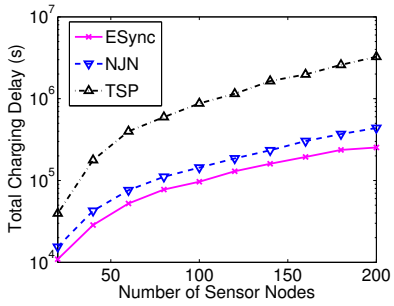

(b) Total charging delay

Figure 14: Impact of nodes number n.

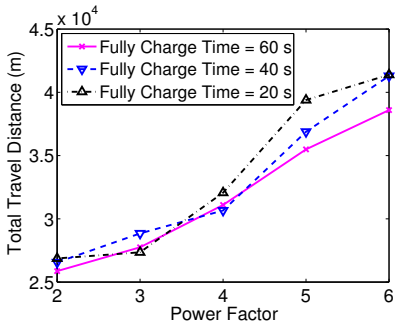

(a) Total travel distance

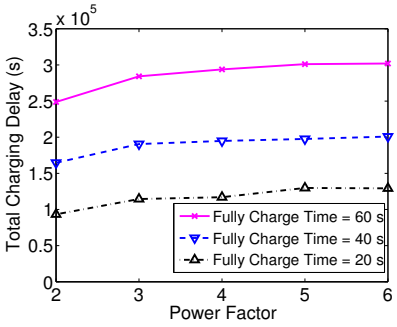

(b) Total charging delay

Figure 15: Impact of power factor α.

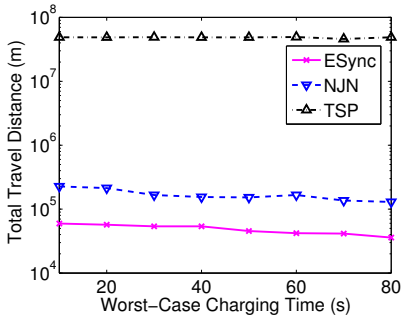

(a) Total travel distance

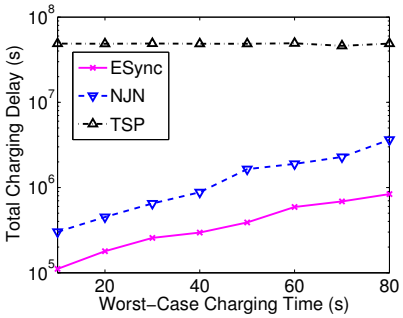

(b) Total charging delay

Figure 16: With random consumptions.

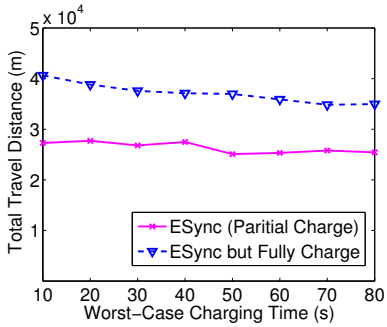

(a) Total travel distance

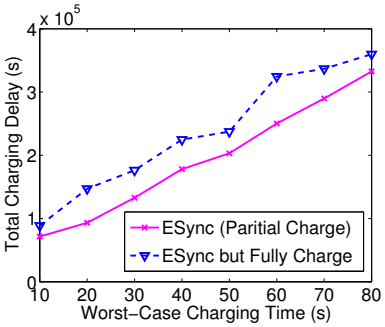

(b) Total charging delay

Figure 17: Advantage of partial charging.

delay of nodes) resultant with *ESync* is about 58.78% (67.11%) of that returned by Nearest-Job-Next when 100 nodes are deployed. When compared with TSP, the two ratios are further reduced to 11.73% and 11.03% respectively. The charging performance degrades as the network scale increases. Thus multiple chargers may be needed in large-scale networks. We will further investigate the collaborative mobile charging process in our future work.

7.3.2 *Impact of Power Factor*

From our simulation results, we observe that a power factor of 2 is adopted for most of the time. To further investigate the impact of α, we fix the network scale at 100 nodes in a 100 $m \times 100$ m field, and explore *ESync* with α varying from 2 to 6. The results are shown in Fig. 15(a) and Fig. 15(b). A clear increasing trend of the travel distance and the charging delay can be observed as α becomes larger, which agrees with our observation, and thus validates our method in determining the optimal α.

7.3.3 *Energy Spatial Randomness*

It is intuitive that for multi-hop sensor networks where the sink is located at the center, *ESync* achieves promising performance because nodes near the sink have higher energy consumption rates. To investigate whether *ESync* performs well in networks without this spatial-correlated energy consumption pattern, we modify the simulation by randomly generating nodes energy consumption rates, and the results returned by *ESync*, Nearest-Job-Next, and TSP are shown in Fig. 16(a) and Fig. 16(b). We can see that even when nodes energy consumptions are irrelevant with their spatial locations, *ESync* still outperforms Nearest-Job-Next and TSP significantly. The advantages of *ESync* over different network scenarios verify its versatility.

7.3.4 *Ratio of Partial Charging*

To facilitate the energy synchronization, sometimes nodes may be only partially charged. To investigate whether this occasionally partially charging of nodes degrades the overall charging performance when compared with always fully charging nodes, we modify *ESync* by making the charger always charge sensor nodes to their full capacity, and compare the resultant charging performance with that obtained by the proposed *ESync*. The results are shown in Fig. 17(a) and Fig. 17(b). We can see that although only a small ratio of the requesting nodes are partially charged, they can sig-

nificantly improve the charging performance when compared with always fully charging. Specifically, the charger travel distance and the charging delay of nodes are reduced by around 25% and 20%, respectively.

8. CONCLUSIONS

In this paper, we have proposed *ESync*, a novel mobile charging protocol for rechargeable sensor networks. Observing the inefficiency of the classic TSP-based mobile charging solutions, we have proposed a *power-*α clustering algorithm to cluster nodes based on their energy consumption rates and then a set of nested optimal T-SP tours is constructed accordingly. A tour selection algorithm has been presented accordingly. As a result, only energy-hungry nodes are involved in the selected TSP tour in each charging round, and thus the charger travel distance is reduced. Furthermore, we proactively adjust the requests sequence of sensor nodes to synchronize it with the selected TSP tour in each charging round, which reduces the charging delay of sensor nodes. The efficiency of *ESync* is verified through both experiments and simulations.

Acknowledgment: This research was supported in part by iTrust IGDSi1305013, SUTD-ZJU/RES/03/2011, Singapore-MIT International Design Center IDG31000101, NSFC 61222305, NSERC Canada, ZJNSF LY14F030016, and National Program for Special Support of Top-Notch Young Professionals.

9. REFERENCES

[1] D. Chu, N. D. Lane, T. Lai, C. Pang, X. Meng, Q. Guo, F. Li, and F. Zhao, "Balancing energy, latency and accuracy for mobile sensor data classification," in *SenSys'11*, 2011.

[2] T. Park, J. Lee, I. Hwang, C. Yoo, L. Nachman, and J. Song, "E-gesture: A collaborative architecture for energy-efficient gesture recognition with hand-worn sensor and mobile devices," in *SenSys'11*, 2011.

[3] Y. Wang, R. Tan, G. Xing, X. Tan, J. Wang, and R. Zhou, "Spatiotemporal aquatic field reconstruction using robotic sensor swarm," in *RTSS'12*, 2012.

[4] X. Wang, S. Han, Y. Wu, and X. Wang, "Coverage and energy consumption control in mobile heterogeneous wireless sensor networks," *IEEE Transactions on Automatic Control*, vol. 58, no. 4, pp. 975–988, 2013.

[5] X. Mao, S. Tang, X. Xu, X.-Y. Li, and H. Ma, "Energy-efficient opportunistic routing in wireless sensor networks," *Parallel and Distributed Systems, IEEE Transactions on*, vol. 22, no. 11, pp. 1934–1942, 2011.

[6] K. Han, L. Xiang, J. Luo, and Y. Liu, "Minimum-Energy Connected Coverage in Wireless Sensor Networks with Omni-Directional and Directional Features," in *Proc. of the 13th ACM/SIGMOBILE Symposium on Mobile Ad Hoc Networking & Computing (MobiHoc'12)*, 2012, p. 85ą94.

[7] Z. Li, Y. Peng, W. Zhang, and D. Qiao, "J-roc: a joint routing and charging scheme to prolong sensor network lifetime," in *ICNP'11*, 2011.

[8] Y. Peng, Z. Li, W. Zhang, and D. Qiao, "Prolonging sensor network lifetime through wireless charging," in *RTSS'10*, 2010.

[9] S. Zhang, J. Wu, and S. Lu, "Collaborative mobile charging," *IEEE Transactions on Computers*, to appear.

[10] Y. Shi, L. Xie, Y. T. Hou, and H. D. Sherali, "On renewable sensor networks with wireless energy transfer," in *INFOCOM'11*, 2011.

[11] L. Fu, P. Cheng, Y. Gu, J. Chen, and T. He, "Minimizing Charging Delay in Wireless Rechargeable Sensor Networks," in *INFOCOM'13*, 2013.

[12] L. He, Y. Gu, and T. He, "Poster abstract: Energy synchronized charging in sensor networks," in *SenSys'12*, 2012.

[13] C. Park and P. Chou, "Ambimax: autonomous energy harvesting platform for multi-supply wireless sensor nodes," in *SECON'06*, 2006.

[14] M. Gorlatova, P. Kinget, I. K. and D. Rubenstein, X. Wang, and G. Zussman, "Challenge: ultra-low-power energy-harvesting active networked tags (EnHANTs)," in *MOBICOM'09*, 2009.

[15] A. Kansal, J. Hsu, S. Zahedi, and M. Srivastava, "Power management in energy harvesting sensor networks," *ACM TECS*, vol. 6, no. 4, 2007.

[16] T. Zhu, Z. Zhong, Y. Gu, T. He, and Z.-L. Zhang, "Leakage-aware energy synchronization for wireless sensor networks," in *MOBISYS'09*, 2009.

[17] T. Zhu, Y. Gu, T. He, and Z. Zhang, "eShare: a capacitor-driven energy storage and sharing network for long-term operation," in *SenSys'10*, 2010.

[18] L. Xie, Y. Shi, Y. T. Hou, W. Lou, H. D. Serali, and S. F. Midkiff, "On renewable sensor networks with wireless energy transfer: The multi-node case," in *SECON'12*, 2012.

[19] B. Tong, Z. Li, G. Wang, and W. Zhang, "How wireless power charging technology affects sensor network deployment and routing," in *ICDCS'10*, 2010.

[20] M. Zhao, J. Li, and Y. Yang, "Joint mobile energy replenishment and data gathering in wireless rechargeable sensor networks," in *ITC'11*, 2011.

[21] L. Xie, Y. Shi, Y. T. Hou, W. Lou, and H. D. Serali, "On traveling path and related problems for a mobile station in a rechargeable sensor network," in *MobiHoc'13*, 2013.

[22] J. Li, C. Wang, F. Ye, and Y. Yang, "Netwrap: An NDN based real time wireless recharging framework for wireless sensor networks," in *Mobile Ad-Hoc and Sensor Systems (MASS), 2013 IEEE 10th International Conference on*, 2013, pp. 173–181.

[23] E. Altman and H. Levy, "Queueing in space," *Advances in Applied Probability*, vol. 26, no. 4, pp. pp. 1095–1116, 1994.

[24] J. Bertsimas and G. V. Ryzins, "A stochastic and dynamic vehicle routing problem in the Euclidean plane," *Operations Research*, vol. 39, 1991.

[25] "Supercapacitors," http://batteryuniversity.com.

[26] B. P. Wells, "Series resonant inductive charging circuit," in *U. S. Patent 6 972 543*, 2005.

[27] X. Liu, H. Zhao, X. Yang, X. Li, and N. Wang, "Trailing mobile sinks: a proactive data reporting protocol for wireless sensor networks," in *MASS'10*, 2010.

[28] V. Kulathumani, A. Arora, M. Sridharan, and M. Demirbas, "Trail: a distance-sensitive sensor network service for distributed object tracking," *ACM Trans. on Sens. Net.*, vol. 5, no. 2, 2009.

[29] G. Xing, T. Wang, W. Jia, and M. Li, "Rendezvous design algorithms for wireless sensor networks with a mobile base station," in *MOBIHOC'08*, 2008.

[30] "Intel Berkeley Research Lab Data," http://www.select.cs.cmu.edu/data/labapp3/index.html.

[31] "Concorde TSP Solder," http://www.tsp.gatech.edu/concorde.html.

[32] Y. Wang, M. C. Vuran, and S. Goddard, "Stochastic analysis of energy consumption in wireless sensor networks," in *SECON'10*, 2010.

[33] H. Sabbineni and K. Chakrabarty, "Data collection in event-driven wireless sensor networks with mobile sinks," *International Journal of Distributed Sensor Networks*, vol. 2010, 2010.

[34] X. Jiang, P. Dutta, D. Culler, and I. Stoica, "Micro power meter for energy monitoring of wireless sensor networks at scale," in *IPSN'07*, 2007.

[35] V. Shnayder, M. Hempstead, B. R. Chen, G. W. Allen, and M. Welsh, "Simulating the power consumption of large-scale sensor network applications," in *SenSys'04*, 2004.

[36] "NCR18650," http://www.panasonic.com.

[37] "Elixir II," https://play.google.com/store/apps/.

[38] O. Gnawali, R. Fonseca, K. Jamieson, D. Moss, and P. Levis, "Collection Tree Protocol," in *SenSys'09*, November 2009.